Hindawi Publishing Corporation
International Journal of Photoenergy
Volume 2012, Article ID 461291, 5 pages
doi:10.1155/2012/461291

*Research Article*

# Synthesis and Photocatalytic Properties of One-Dimensional Composite $Bi_2O_3$-$Bi_2CrO_6$ Nanowires

**Qianqian Zhang,[1] Baibiao Huang,[2] Peng Wang,[2] Xiaoyang Zhang,[2] Xiaoyan Qin,[2] and zeyan wang[2]**

[1] *School of Chemistry and Chemical Engineering, Shandong University, Jinan 250100, China*
[2] *State Key Laboratory of Crystal Materials, Shandong University, Jinan 250100, China*

Correspondence should be addressed to Baibiao Huang, bbhuang@sdu.edu.cn

Received 11 July 2012; Accepted 29 July 2012

Academic Editor: Jiaguo Yu



One-dimensional composite $Bi_2O_3$-$Bi_2CrO_6$ nanowires were successfully fabricated by a simple microwave-assistant hydrothermal method. The successful fabrication of one-dimensional $Bi_2O_3$-$Bi_2CrO_6$ nanowires can only be realized at pH value range of 1–5 of the starting solution. The fabricated nanowires were characterized by X-ray powder diffraction (XRD), scanning electron microscope (SEM), transmission electron microscopy (TEM), UV-visible diffuse reflectance spectra (UV-Vis DRS), and photoluminescence (PL), respectively. The diameter of the nanowires varies from 30 to 100 nm; the length is a few micrometers. Methylene blue (MB) solutions were used to evaluate the visible light photocatalytic activities of the fabricated samples. Compared with $Bi_2O_3$, the fabricated $Bi_2O_3$-$Bi_2CrO_6$ nanowires show enhanced efficiency in oxidization of MB under visible light.

## 1. Introduction

One-dimensional nanostructures with distinctive structures and properties play important roles in nanotechnology for their use as building blocks in nanoscale circuits, optoelectronic, electrochemical, and electromechanical devices [1, 2]. The synthesis of one-dimensional (1D) nanostructures [3–7] has gained tremendous amount of attention in recent years due to their fascinating sizes, shapes, and material-dependent properties. Nanotubes, nanobelts, nanorods, and semiconducting nanowires have been fabricated through a number of advanced nanolithographic techniques, thermal evaporations, and solution-based methods [8–11]. Among all the one-dimensional nanostructures, the composite nanowires with two different constitutions are widely investigated [12, 13]. Vomiero et al. produced radial and longitudinal nanosized $In_2O_3$-$SnO_2$ by applying a suitable methodology of transport and condensation [14]. Bachas's group has synthesized a new class of bimetallic nanotubes based on Pd/Fe and demonstrated their efficacy in the dechlorination of PCB 77 (a polychlorinated biphenyl) one-dimensional iron metal nanotubes of different diameters were prepared by electroless deposition within the pores of PVP-coated polycarbonate membranes using a simple technique under ambient conditions. The longitudinal nucleation of the nanotubes along the pore walls was achieved by mounting the PC membrane between two halves of a U-shape reaction tube [15]. Coaxial $SnO_2$@TNTs, with two-fold tubular structures, are assembled by electrochemical and solvothermal embedments of $SnO_2$ nanolayers inside the pristine $TiO_2$ nanotube arrays. The excellent electrochemical properties originated from the synergistic effect with improved electronic conductivity and dual lithium storage mechanism, demonstrating that the coaxial $SnO_2$@TNT hybrid is a promising candidate for electrochemical energy storage [16]. In case of our research, microwave hydrothermal method was employed in the fabrication process. Microwave irradiation provides rapid and uniform heating of reagents and solvents [17–19]. The rapid microwave heating provides uniform nucleation and growth conditions, which conduce to homogeneous and well crystalline nanomaterials. We demonstrate a simple and efficient approach to synthesize one-dimensional nanowires

within 60 min of microwave irradiation. During the process, no organic surfactant and catalyst were used. The time and energy consumption were saved with the microwave route of syntheses. Comparative experiment was carried out the same reaction time by common hydrothermal method while keeping other synthetic parameters in same. No nanowire was obtained.

Bismuth-containing oxides have been extensively studied because of their interesting properties, including ferroelectricities [20], ionic conductivities [21], superconductivities [22], and catalytic activities [23]. As a photocatalyst [24, 25], the conduction and valence band edges of $Bi_2O_3$ are +0.33 and +3.13 V relative to NHE, respectively. The band structure of $Bi_2O_3$ accounts for its ability to oxidize organic pollution and generate highly reactive species, such as $O^-\bullet$ and $OH\bullet$ radicals. Although the $Bi_2O_3$ have the proper band structure, the efficiency to decompose organic pollution is still low. In order to improve the photocatalytic ability of $Bi_2O_3$, $Bi_2CrO_6$ was connected to $Bi_2O_3$. $Bi_2CrO_6$ is a novel material with narrow band gap. Upon connection of $Bi_2CrO_6$ to $Bi_2O_3$ nanowires, a unique semiconductor—semiconductor nanoscale contact can be prepared, which shows different properties from $Bi_2O_3$. In this paper, the $Bi_2O_3$ and $Bi_2CrO_6$ were synthesized synchronously in the same Teflon autoclave, $Bi_2O_3$ and $Bi_2CrO_6$ are in well contact, and the photogenerated electron and holes can migrate from each other freely. Compared with $Bi_2O_3$, the $Bi_2O_3$-$Bi_2CrO_6$ nanowires show enhanced efficiency in photodegradation of methylic blue under visible light.

## 2. Experimental Section

Analytic grade Bismuth nitrate ($Bi(NO_3)_3$), sodium chromate ($Na_2CrO_4$), sodium hydroxide (NaOH), and hydrochloric acid (HCl) were used as received without any treatment. In a typical procedure, solutions of $Bi(NO_3)_3$ and solutions of $Na_2CrO_4$ in water were prepared as stock solutions in advance. 10 mL of 0.2 M $Bi(NO_3)_3$ stock solution was mixed with 10 mL of 0.1 M $Na_2CrO_4$ aqueous solution, and 1 M HCl solution was added to adjust the pH value of the mixed solution to 3. The solution was magnetically stirred for about 0.5 h, then transferred into a special Teflon autoclave, and heated at 180°C for 1 h under microwave radiation. The resulting precipitate was collected, washed with dilute HCl aqueous solution and deionized water until the pH value of the washing solution was about 7, and dried in air at 80°C for 8 h.

X-ray powder diffraction (XRD) patterns were obtained by a Bruker AXS D8 advance powder diffractometer. The scanning electron microscope (SEM) image of the products was examined by a Hitachi, S-4800 microscope. Transmission electron microscopy (TEM) was performed with a HITACH H-600 Electron Microscope. The UV-visible diffuse reflectance spectrum was obtained by Shimadzu UV-2550. PL spectrum measurement was performed in a fluorescence spectrophotometer (Edinburgh, FL920) at room temperature. A reference photocatalyst $Bi_2O_3$ was prepared using the method reported in the literature [24].

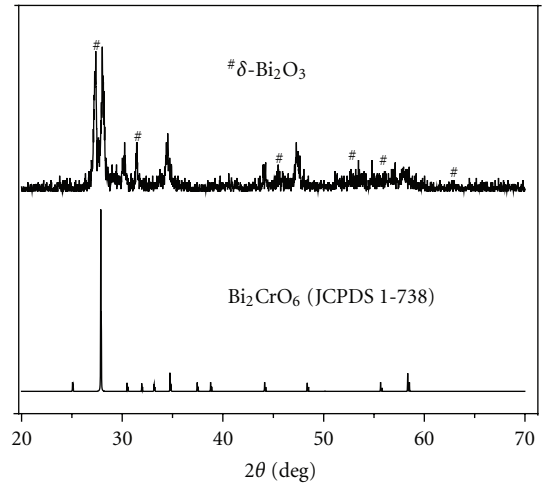


Figure 1: XRD pattern of the composite $Bi_2O_3$-$Bi_2CrO_6$ nanowires.

Photocatalytic activities of $Bi_2O_3$-$Bi_2CrO_6$ were evaluated by studying degradation of methylic blue (MB) dye. The photocatalytic degradation of MB dye was carried out with 0.2 g of the powdered photocatalyst suspended in 100 mL solution of MB dye prepared by dissolving 20 mg of MB powder in 1 L of distilled water in a Pyrex glass cell at room temperature under air. The optical system for detecting the catalytic reaction included a 300 W Xe arc lamp (focused through a shutter window, Chang Tuo, Beijing) with UV cutoff filter (providing visible light $\lambda \geq 400$ nm).

## 3. Results and Discussion

A powder XRD pattern (Figure 1) of the product initially suggests the coexistence of $Bi_2O_3$ (JCPDS file 16-654) and $Bi_2CrO_6$ (JCPDS file 1-738). The peaks in this figure can be indexed to a cubic phase of $Bi_2O_3$ (space group Fm-3 m (no. 225)) with lattice constants $a = 5.66$ Å. The system and lattice constants of $Bi_2CrO_6$ are not shown in the Joint Committee on Powder Diffraction Standards card. Figure 2 shows SEM images of $Bi_2O_3$-$Bi_2CrO_6$ nanowire. The diameter of the nanowires is about 30–100 nm, and the length is in the range of micrometers. The morphology of the nanowire is uniform.

Typical TEM images of $Bi_2O_3$-$Bi_2CrO_6$ nanowires are shown in Figures 3(a) and 3(b). According to Figure 3(a), the diameter of the nanowires varies from 30 to 100 nm, the length is a few micrometers, which is consistent with SEM results. Figure 3(b) shows TEM micrograph of a typical nanowire junction. The knots can be clearly seen in the nanowire structures. The interval between two knots is not equal and ranges from several ten to hundred of nanometers.

UV-visible diffuse reflectance spectra of commercial $Bi_2O_3$, fabricated $Bi_2O_3$ and the composite $Bi_2O_3$-$Bi_2CrO_6$ nanowires are shown in Figure 4. It can be seen that the absorbance of $Bi_2O_3$-$Bi_2CrO_6$ nanowire extends to the visible light region. The onset of the adsorption edge is 515 nm in the UV-vis diffuse reflectance spectrum. The nanowire can absorb light with wavelength $\lambda < 515$ nm, covering the region from UV through near visible light in the sunlight,

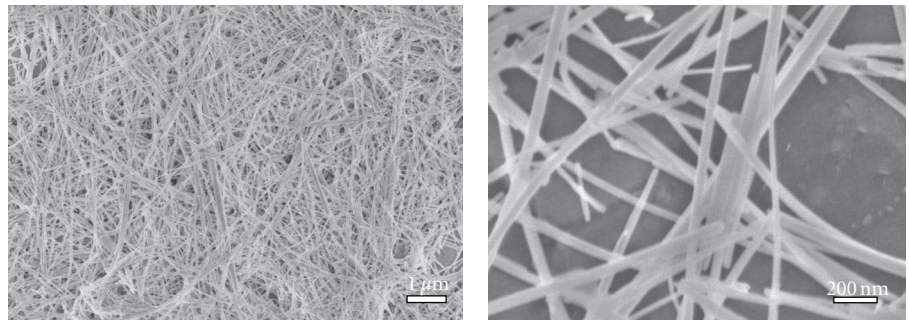


(a) (b)

Figure 2: SEM images of the composite $Bi_2O_3$-$Bi_2CrO_6$ nanowires: (a) low magnification; (b) high magnification.

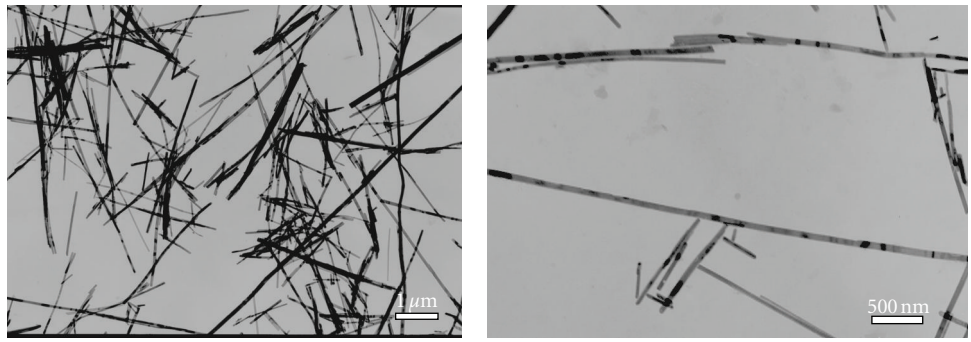


(a) (b)

Figure 3: (a) TEM image of the composite $Bi_2O_3$-$Bi_2CrO_6$ nanowires; (b) a TEM image of a typical nanowire junction.

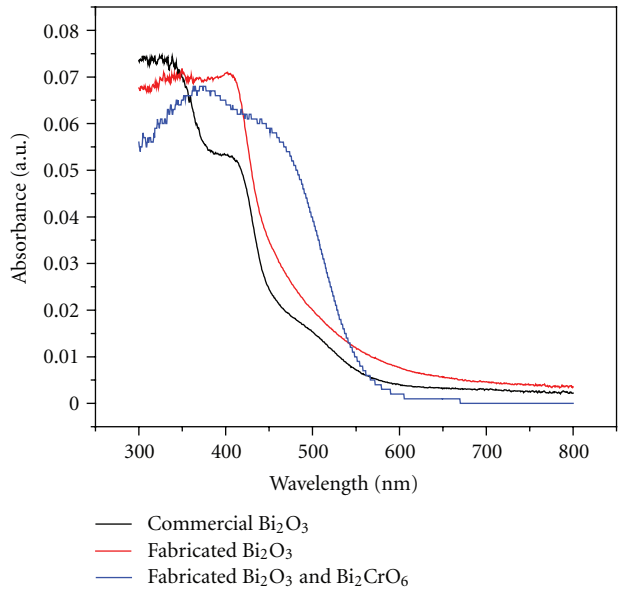


Figure 4: The UV-visible diffuse reflectance spectra of commercial $Bi_2O_3$, fabricated $Bi_2O_3$, and the composite $Bi_2O_3$-$Bi_2CrO_6$ nanowires.

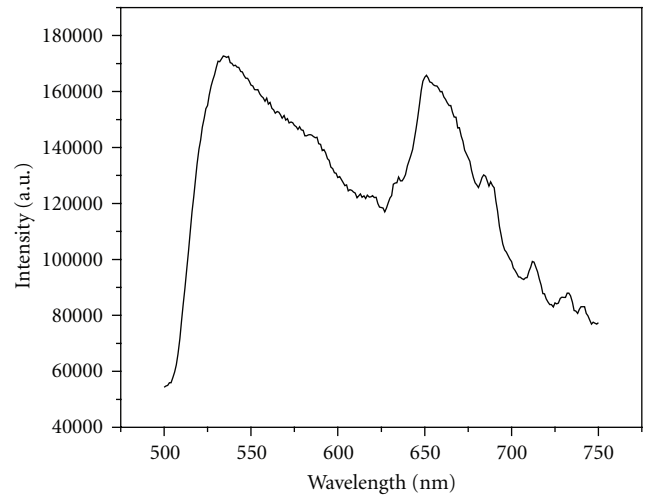


Figure 5: The PL spectrum of the composite $Bi_2O_3$-$Bi_2CrO_6$ nanowires.

and can be used as a visible light photocatalyst to decompose the organic pollution. Compared with commercial and fabricated $Bi_2O_3$, the light absorption of $Bi_2O_3$-$Bi_2CrO_6$ in 440 nm to 540 nm is strongest. The PL spectrum of the sample is presented in Figure 5. Two peaks, 535 and 651 nm in the PL spectrum can be seen, which meant two recombined semiconductors. Both of them are in visible light region; one is attributed to $Bi_2O_3$, and the other is due to $Bi_2CrO_6$. The excitation wavelength was set at 430 nm.

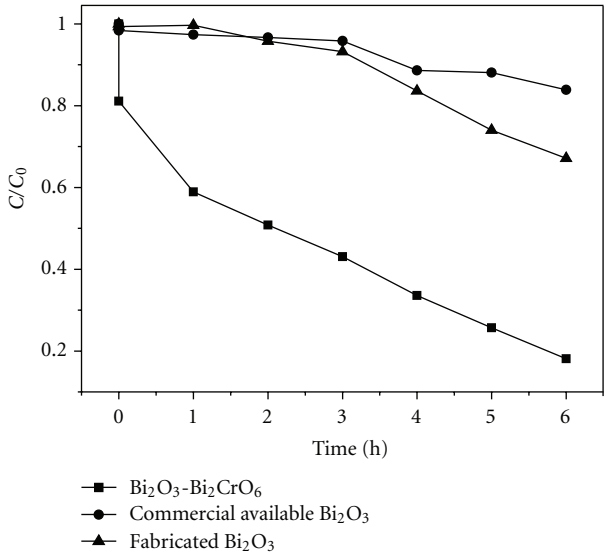


Figure 6: Photodecomposition of MB dye in solution (20 mg/L) over $Bi_2O_3$-$Bi_2CrO_6$ composite nanowires, commercial available $Bi_2O_3$ and fabricated $Bi_2O_3$, under visible-light irradiation ($\lambda \geq 400$ nm). $C$ is the concentration of MB dye at time $t$, and $C_0$ is the original concentration before it is irradiated.

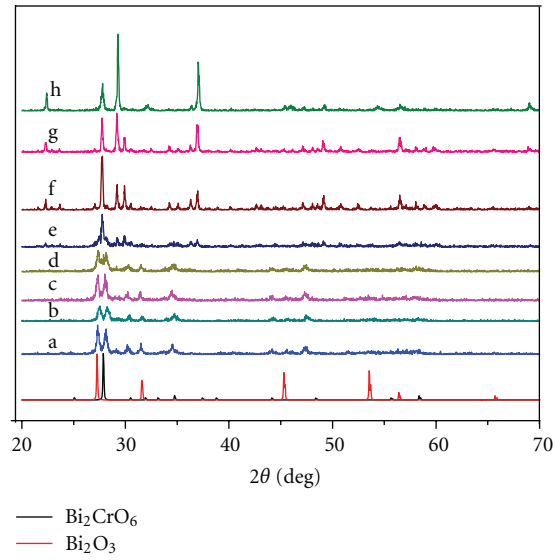


Figure 7: XRD pattern of the sample synthesized in different pH value of starting solution: (a) pH = 1; (b) pH = 2; (c) pH = 3; (d) pH = 4; (e) pH = 5; (f) pH = 6; (g) pH = 7; (h) pH = 11.

To probe the photocatalytic activity of the composite $Bi_2O_3$-$Bi_2CrO_6$ nanowire in visible part of the solar spectrum, the bleaching of MB was carried out under irradiation of a Xe arc lamp with UV cutoff filter (providing visible light $\lambda \geq 400$ nm). An aliquot (2 mL) of MB solution was removed at interval times and placed in the UV-vis spectrometer for analysis. The results were shown in Figure 6. As shown in Figure 6, the photocatalytic activity of $Bi_2O_3$-$Bi_2CrO_6$ nanowires is higher than fabricated $Bi_2O_3$ and the commercial available $Bi_2O_3$; more than 82% of MB molecules were decomposed in 6 h, while the reference photocatalysts $Bi_2O_3$ and the commercial available $Bi_2O_3$, only 33% and 17% of the MB dye, were decomposed in 6 h, respectively. (As pure $Bi_2CrO_6$ phase cannot be obtained, so we just choose the $Bi_2O_3$ as the reference photocatalysts.) The valence band of $Bi_2O_3$ is composed of O2p, and the conduction band is consisted of Bi5d. The import of Cr element leads to the band positions of $Bi_2CrO_6$ different from the band positions of $Bi_2O_3$. (Since the pure $Bi_2CrO_6$ phase and the crystal structure and lattice constants of $Bi_2CrO_6$ cannot be obtained, we cannot use the plane-wave-based density functional method to clarify whether $Cr^{6+}$ contributed to valence- or conduction-band formation in $Bi_2CrO_6$). The photogenerated electrons and holes can transfer between $Bi_2O_3$ and $Bi_2CrO_6$, the different band positions of $Bi_2O_3$ and $Bi_2CrO_6$, enhance the separation of photogenerated electrons and holes, leading to higher efficiency in degradation of MB.

The successful fabrication of one-dimensional composite $Bi_2O_3$-$Bi_2CrO_6$ nanowires can only be realized at the pH value range of 1–5 of starting solution. Comparative experiments were made by adjusting the starting solution's pH value 6, 7, and 11 while keeping other synthetic parameters in the same condition. Figure 7 shows the XRD pattern of as-synthesized products. The XRD measurements show that the composition and structure changed drastically along with the increasing of the pH value. Below pH 5, the XRD pattern exhibits the product is composed of $Bi_2O_3$ (JCPDS file 16–654) and $Bi_2CrO_6$ (JCPDS file 1-738). The peaks belonged to $Bi_2O_3$ and $Bi_2CrO_6$ become weakened till disappeared, and subsequent peaks of newly formed crystals structure start to emerge above pH 5. At pH 11, the sample is mainly composed of $Bi_2O_{2.33}$ (JCPDS file 27-51), $Bi(OH)_3$ (JCPDS file 1-898), and CrOOH (JCPDS file 70-1115). Seen from Figure 7, the pH values of the starting solution greatly affect the fabrication of composite $Bi_2O_3$-$Bi_2CrO_6$ nanowires, and the composite $Bi_2O_3$-$Bi_2CrO_6$ nanowires can be obtained at starting solution's pH value below 5.

In conclusion, one-dimensional $Bi_2O_3$-$Bi_2CrO_6$ nanowires were synthesized by a simple microwave-assistant hydrothermal method. The diameter of the wires is about 30–100 nm, and the length is in range of micrometers. The sample can absorb visible light ($\lambda < 515$ nm), covering the region from UV through near visible light in the sunlight, showing high efficiency in degradation of MB under visible light irradiation. The work of $Bi_2O_3$-$Bi_2CrO_6$ nanowires on water splitting is still in process.

## Acknowledgments

This work is financially supported by the National Basic Research Program of China (973 Program, Grant 2007CB613302), the National Natural Science Foundation of China under Grants 20973102, 51021062, 51002091, and 21007031. The authors also express thanks for editor's patience.

## References


[1] J. Li, Y. Zhang, S. To, L. You, and Y. Sun, "Effect of nanowire number, diameter, and doping density on nano-FET biosensor sensitivity," *ACS Nano*, vol. 5, no. 8, pp. 6661–6668, 2011.

[2] A. R. Rathmell, M. Nguyen, M. Chi, and B. J. Wiley, "Synthesis of oxidation-resistant cupronickel nanowires for transparent conducting nanowire networks," *Nano Letters*, vol. 12, no. 6, pp. 3193–3199, 2012.

[3] S. Deng, V. Tjoa, H. M. Fan et al., "Reduced graphene oxide conjugated $Cu_2O$ nanowire mesocrystals for high-performance $NO_2$ gas sensor," *Journal of the American Chemical Society*, vol. 134, no. 10, pp. 4905–4917, 2012.

[4] S. Hoang, S. P. Berglund, N. T. Hahn, A. J. Bard, and C. B. Mullins, "Enhancing visible light photo-oxidation of water with $TiO_2$ nanowire arrays via cotreatment with $H_2$ and $NH_3$: synergistic effects between $Ti^{3+}$ and N," *Journal of the American Chemical Society*, vol. 134, no. 8, pp. 3659–3662, 2012.

[5] H. W. Liang, S. Liu, and S. H. Yu, "Controlled synthesis of one-dimensional inorganic nanostructures using pre-existing one-dimensional nanostructures as templates," *Advanced Materials*, vol. 22, no. 35, pp. 3925–3937, 2010.

[6] H. Huang, B. Liang, Z. Liu, X. Wang, D. Chen, and G. Shen, "Metal oxide nanowire transistors," *Journal of Materials Chemistry*, vol. 22, no. 27, pp. 13428–13445, 2012.

[7] J. J. Hill, N. Banks, K. Haller, M. E. Orazem, and K. J. Ziegler, "An interfacial and bulk charge transport model for dye-sensitized solar cells based on photoanodes consisting of core-shell nanowire arrays," *Journal of the American Chemical Society*, vol. 133, no. 46, pp. 18663–18672, 2011.

[8] H. Geaney, C. Dickinson, C. A. Barrett, and K. M. Ryan, "High density germanium nanowire growth directly from copper foil by self-induced solid seeding," *Chemistry of Materials*, vol. 23, no. 21, pp. 4838–4843, 2011.

[9] J. Z. Liu, P. X. Yan, G. H. Yue, L. B. Kong, R. F. Zhuo, and D. M. Qu, "Synthesis of doped ZnS one-dimensional nanostructures via chemical vapor deposition," *Materials Letters*, vol. 60, no. 29-30, pp. 3471–3476, 2006.

[10] F. Wang, A. Dong, J. Sun, R. Tang, H. Yu, and W. E. Buhro, "Solution-liquid-solid growth of semiconductor nanowires," *Inorganic Chemistry*, vol. 45, no. 19, pp. 7511–7521, 2006.

[11] K. Li, H. Wang, C. Pan, J. Wei, R. Xiong, and J. Shi, "Enhanced photoactivity of Fe + N Codoped anatase-rutile $TiO_2$ nanowire film under visible light irradiation," *International Journal of Photoenergy*, vol. 2012, Article ID 398508, 8 pages, 2012.

[12] Z. Liu, D. D. Sun, P. Guo, and J. O. Leckie, "An efficient bicomponent $TiO_2/SnO_2$ nanofiber photocatalyst fabricated by electrospinning with a side-by-side dual spinneret method," *Nano Letters*, vol. 7, no. 4, pp. 1081–1085, 2007.

[13] M. Müllner, T. Lunkenbein, J. Breu, F. Caruso, and A. H. E. Müller, "Template-directed synthesis of silica nanowires and nanotubes from cylindrical core-shell polymer brushes," *Chemistry of Materials*, vol. 24, no. 10, pp. 1802–1810, 2012.

[14] A. Vomiero, M. Ferroni, E. Comini, G. Faglia, and G. Sberveglieri, "Preparation of radial and longitudinal nanosized heterostructures of $In_2O_3$ and $SnO_2$," *Nano Letters*, vol. 7, no. 12, pp. 3553–3558, 2007.

[15] E. M. Zahran, D. Bhattacharyya, and L. G. Bachas, "Development of reactive Pd/Fe bimetallic nanotubes for dechlorination reactions," *Journal of Materials Chemistry*, vol. 21, no. 28, pp. 10454–10462, 2011.

[16] X. Wu, S. Zhang, L. Wang et al., "Coaxial $SnO_2$@$TiO_2$ nanotube hybrids: from robust assembly strategies to potential application in $Li^+$ storage," *Journal of Materials Chemistry*, vol. 22, no. 22, pp. 11151–11158, 2012.

[17] M. N. Nadagouda and R. S. Varma, "Microwave-assisted synthesis of crosslinked poly(vinyl alcohol) nanocomposites comprising single-walled carbon nanotubes, multi-walled carbon nanotubes, and buckminsterfullerene," *Macromolecular Rapid Communications*, vol. 28, no. 7, pp. 842–847, 2007.

[18] R. S. Varma, *Microwaves in Organic Synthesis*, chapter 8, Wiley-VCH, Weinheim, Germany, 2006.

[19] Z. P. Qiao, Y. Zhang, L. T. Zhou, and Q. Xire, "Shape control of PbS crystals under microwave irradiation," *Crystal Growth and Design*, vol. 7, no. 12, pp. 2394–2396, 2007.

[20] R. V. K. Mangalam, P. Mandal, E. Suard, and A. Sundaresan, "Ferroelectricity in ordered perovskite $BaBi_{0.5}{}^{3+}(Bi_{0.2}{}^{5+}Nb_{0.3}{}^{5+})O_3$ with $Bi^{3+}$:$6s^2$ lone pair at the B-site," *Chemistry of Materials*, vol. 19, no. 17, pp. 4114–4116, 2007.

[21] F. Mauvy, J. C. Launay, and J. Darriet, "Synthesis, crystal structures and ionic conductivities of $Bi_{14}P_4O_{14}$ and $Bi_{50}V_4O_{85}$. Two members of the series $Bi_{18-4m}M_{4m}O_{27+4m}$ (M=P, V) related to the fluorite-type structure," *Journal of Solid State Chemistry*, vol. 178, no. 6, pp. 2015–2023, 2005.

[22] M. L. Munzarová and R. Hoffmann, "Strong electronic consequences of intercalation in cuprate superconductors: the case of a trigonal planar AuI3 complex stabilized in the $Bi_2Sr_2CaCu_2Oy$ lattice," *Journal of the American Chemical Society*, vol. 124, no. 19, pp. 5542–5549, 2002.

[23] W. J. M. van Well, M. T. Le, N. C. Schiødt, S. Hoste, and P. Stoltze, "The influence of the calcination conditions on the catalytic activity of $Bi_2MoO_6$ in the selective oxidation of propylene to acrolein," *Journal of Molecular Catalysis A*, vol. 256, no. 1-2, pp. 1–8, 2006.

[24] A. Hameed, T. Montini, V. Gombac, and P. Fornasiero, "Surface phases and photocatalytic activity correlation of $Bi_2O_3/Bi_2O_{4-x}$ nanocomposite," *Journal of the American Chemical Society*, vol. 130, no. 30, pp. 9658–9659, 2008.

[25] X. Yong and M. A. A. Schoonen, "The absolute energy positions of conduction and valence bands of selected semiconducting minerals," *American Mineralogist*, vol. 85, no. 3-4, pp. 543–556, 2000.